Deep Water Renewal in the Strait of Georgia

D. Masson

Institute of Ocean Sciences, Sidney, BC, Canada V8L 4B2

The Strait of Georgia is a semi-enclosed basin on the Canadian west coast in which exchange with the shelf is restricted by narrow constrictions and shallow sills. The local dynamics are mostly dominated by the mixed tides and by the estuarine circulation that is forced mainly by discharge of fresh water from the Fraser River. The intermediate and deep water of the Strait are renewed through discrete deep water renewal events during which dense water flows over the sills and into the interior basin. Several data sets are closely examined to better understand the nature and variability of the deep water renewal process over a wide range of time scales. Measured deep water renewal (DWR) events are clearly identified, as well as their effects on the water properties in the deep basin. It is found that the events can be classified into two categories: late winter intrusions bring cold, oxygen rich water, and late summer events bring warm, saline, low oxygen water. These two DWR seasons determine the annual cycle of the deep water properties in the Strait of Georgia.

For both seasons, the DWR events always occur following a neap tide, at which time the density of bottom water in the sill area peaks. However, not all neap tides are followed by a DWR event. During the DWR seasons, discrete events are found to occur every second neap tide. It is believed that this monthly periodicity is required to allow enough time for the salinity (density) of the deep water near the sill to increase sufficiently following the flushing of dense local water by the previous DWR event. Also, the timing of the two DWR seasons is explained in terms of the yearly cycle of the surface and bottom water density in the estuary: DWR events are more likely to happen at the beginning (spring) and end (fall) of the coastal upwelling season, when the Fraser River discharge is not too large. Finally, it is shown that, during El Niño years, unfavorable conditions develop that can shut down the late winter DWR season, leading to much warmer deep water during the following winter.   © 2002 Elsevier Science Ltd.

Introduction

The Strait of Georgia is a large, deep, and fjord-like estuary on the southern coast of British Columbia. It is connected to the Pacific ocean by Juan de Fuca Strait to the south (Figure 1), and by Johnstone Strait to the north. The estuarine circulation is forced mainly by the Fraser River outflow which peaks in early summer at time of maximum snow melt. While the strait is connected to the open ocean on both its northern and southern ends, the northern channel is much more constricted, and most of the estuarine exchange flows through Juan de Fuca Strait. In addition to the freshwater forcing, the circulation in the basin is also influenced by strong tidal currents and wind stress (e.g. Thomson, 1994).

Within the main channel of the coastal system formed by the straits of Georgia and Juan de Fuca, the flow of water is restricted by two major sill areas: the Victoria sill extending across Juan de Fuca south of Victoria, and Boundary Pass (Figure 1). Vigorous mixing is produced in these two shallow areas by the large tidal velocities. In its central section, the Strait of Georgia reaches depths of up to 400 m. For its deep

water mass to be renewed, the estuarine return flow must bring sufficiently dense water over the two sills. This makes the system similar to a fjord with two sills, dividing the coastal system into a set of three basins and making deep water renewal a complex process. In such a system, bottom water intrusions play a dominant role in the replacement of water below sill depth (e.g. Gade & Edwards, 1980).

In an early investigation, Waldichuk (1957) reported that, in the Strait of Georgia, bottom water is formed in late autumn when dense water from Juan de Fuca Strait flows over the southern sills. He also noted that this process is strongly controlled by tidal mixing at the sills. Stacey *et al.* (1987) analysed the low-frequency current fluctuations contained in cyclosonde data collected in the deep Strait of Georgia, from June 1984 to January 1985. Over this period, they found strong, bottom-intensified pulses at fortnightly and monthly periods during which the along-isobath component of velocity reached about 30 cm s^{-1}. These strong pulses were present at one location only (STN3 on Figure 1) and seemed to be confined to within 50 m from the bottom. Unfortunately, the data from the other moorings did not cover water depths
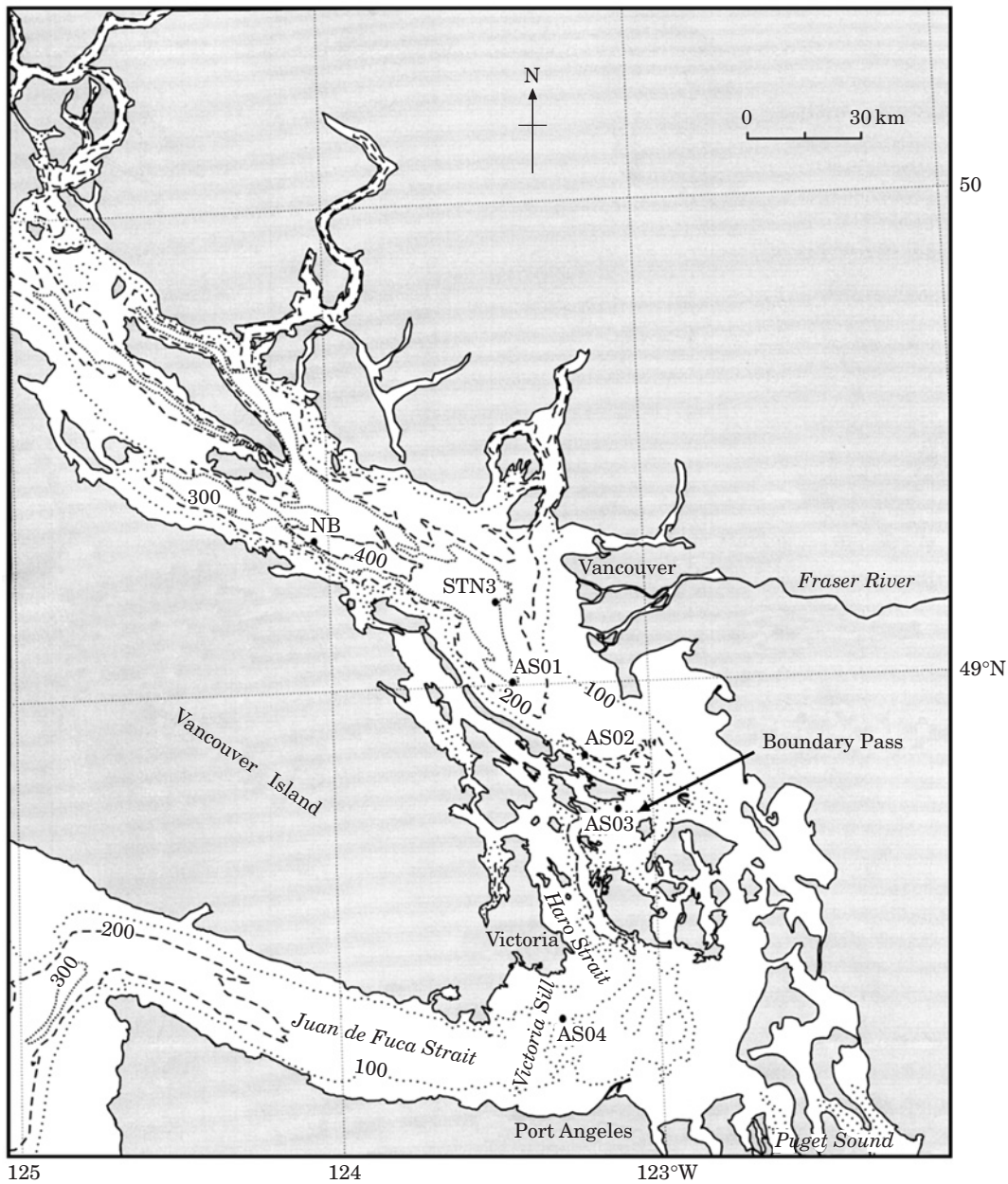
FIGURE 1. The Vancouver Island coastal area including the Straits of Juan de Fuca and Georgia. Also shown are the positions of four current meter moorings, AS01, AS02, AS03, and AS04, along with the long-term hydrographic station of Nanoose Bay, NB, and cyclosonde mooring, STN3.

close enough to the bottom to allow for an estimate of the across-isobath length scale of such events.

LeBlond *et al.* (1991) studied the deep water replacement processes with two different data sets. Based on the 1968 monthly hydrographic survey of Crean and Ages (1971), they found evidence of late winter propagation of cold, brackish and well oxygenated water northwards from Boundary Pass at intermediate depths. They also found some evidence of episodic cold winter intrusions in the deepest layers

of the Strait of Georgia, but the monthly sampling made it difficult to resolve the processes involved. In addition, they examined the same 1984 data set used by Stacey *et al.* (1987) and interpreted the bottom intensified pulses as gravity currents carrying saline water from Juan de Fuca Strait. These pulses apparently originate from Boundary Pass during periods of summer neap tides, and it was suggested that deep penetration is possible only during times of low tidal mixing, when tidal velocities over Boundary

Pass do not exceed a threshold value of about 50 cm s^{-1}.

A numerical modeling study by Marinone and Pond (1996) gives some support to the interpretation of the mechanism for summer deep water renewal in the Strait of Georgia given by LeBlond *et al.* (1991). Their model results show that, during summer neap tides, the water column is able to stratify and a stronger two-layer exchange can be established over the sill, allowing dense water to flow over the sill and sink to the bottom of the strait.

In the Strait of Georgia, DWR events have been previously observed at both intermediate depths and near the bottom. In this paper, only those events reaching the bottom of the deep basin are examined. By detailed analysis of several data sets, we are able to identify various factors and time scales involved in the process. In the next section, DWR events are described using moored current meter measurements collected in 1989–90 at four locations along the thalweg, extending from Victoria sill into the deep central basin of the Strait of Georgia. Two deep water renewal seasons are identified and linked to the yearly cycle of water properties in the deep basin. Section 3 explains the importance of the tidal fortnightly mixing over the sills in the formation of these events. In section 4, the timing of the two DWR seasons is explained in terms of the overlap between the upwelling season on the coast and the Fraser River freshet. Also, the main signal in the year to year variability of the deep water properties is identified as a shutdown of the process during strong El Niño episodes. Finally, conclusions are given in the last section.

Evidence of deep water renewal

To gain some insight into the problem of deep water renewal, a series of current meters were deployed in the Strait of Georgia from June, 1989 to October, 1990 (Birch, 1991). The instruments were positioned 10 m off the bottom at four locations (Figure 1): on Victoria sill (AS04, 90 m depth), in Boundary Pass (AS03, 150 m depth), in the deep trench of the southern Strait of Georgia (AS02, 200 m depth), and within the deep basin of the central strait (AS01, 300 m depth). Because of the strategic placement of the moorings as well as the duration of the deployment, this data set allows a detailed analysis of the deep water renewal process.

In Figure 2(a), density measured near the bottom at AS01, AS02 and AS03 is given for the 1 year period extending from July, 1989 to July, 1990. The time series of density have been lowpass filtered with a 25 h running mean. Large peaks of high density at AS02,

each lasting a few days, indicate 6 distinct deep water renewal events. Each of these dense water pulses is also seen first upstream at AS03, and subsequently landward at AS01. The time lag associated with the passage of the dense pulse at the three stations is only a few days, and, consequently, not clearly evident in the 1 year filtered time series of Figure 2(a). However, examination of the unfiltered time series indicates that the pulses are seen at AS03, AS02 and AS01 successively over a period of a few days, indicative of landward propagation along the thalweg. After each pulse, the local water properties at AS02 eventually return to values close to those measured prior to the event. This is consistent with the idea that each peak of density reflects the passage of a finite pulse of dense water flowing downslope along the bottom from the sill area at Boundary Pass into the deep central basin of the Strait of Georgia.

The accompanying figure [Figure 2(b)] relates the timing of the six dense intrusions (indicated as the time of maximum density measured at AS02) to the evolution over the same period of bottom water temperature and salinity measured near Nanoose Bay, a station located well into the central deep basin of the Strait of Georgia (NB on Figure 1). Vertical profiles have been taken continuously at this location at a rate of a few times per week, since 1969 (1979) for temperature (salinity). Bottom conditions were computed as the mean properties for water depths between 300 m and the bottom at 420 m. Figure 2(b) clearly reveals the importance of deep water renewal in establishing the yearly cycle of water properties in the deep strait. In late summer and early fall, as a succession of bottom intrusions brings in warm salty water, the deep salinity and temperature at the Nanoose Bay station increase to reach maximum values in October. Then, through the following winter, the salinity slowly decreases, and it appears that the deep water mass is gradually mixed with the fresher water above. As for the winter temperature, the vertical gradient is small through most of the water column below the shallow thermocline (Figure 3), and mixing does not change significantly values near the bottom. In the following spring, the last two intrusions indicated in Figure 2(b) are associated with an abrupt decrease in bottom temperature at the Nanoose Bay station. Salinity remains relatively constant because, this time, the incoming water is relatively cold, but with salinities close to ambient values. The bottom temperature typically remains low through the summer until the next series of DWR events occur in early fall.

From the above description, two distinct deep water renewal seasons are identified: the fall season which
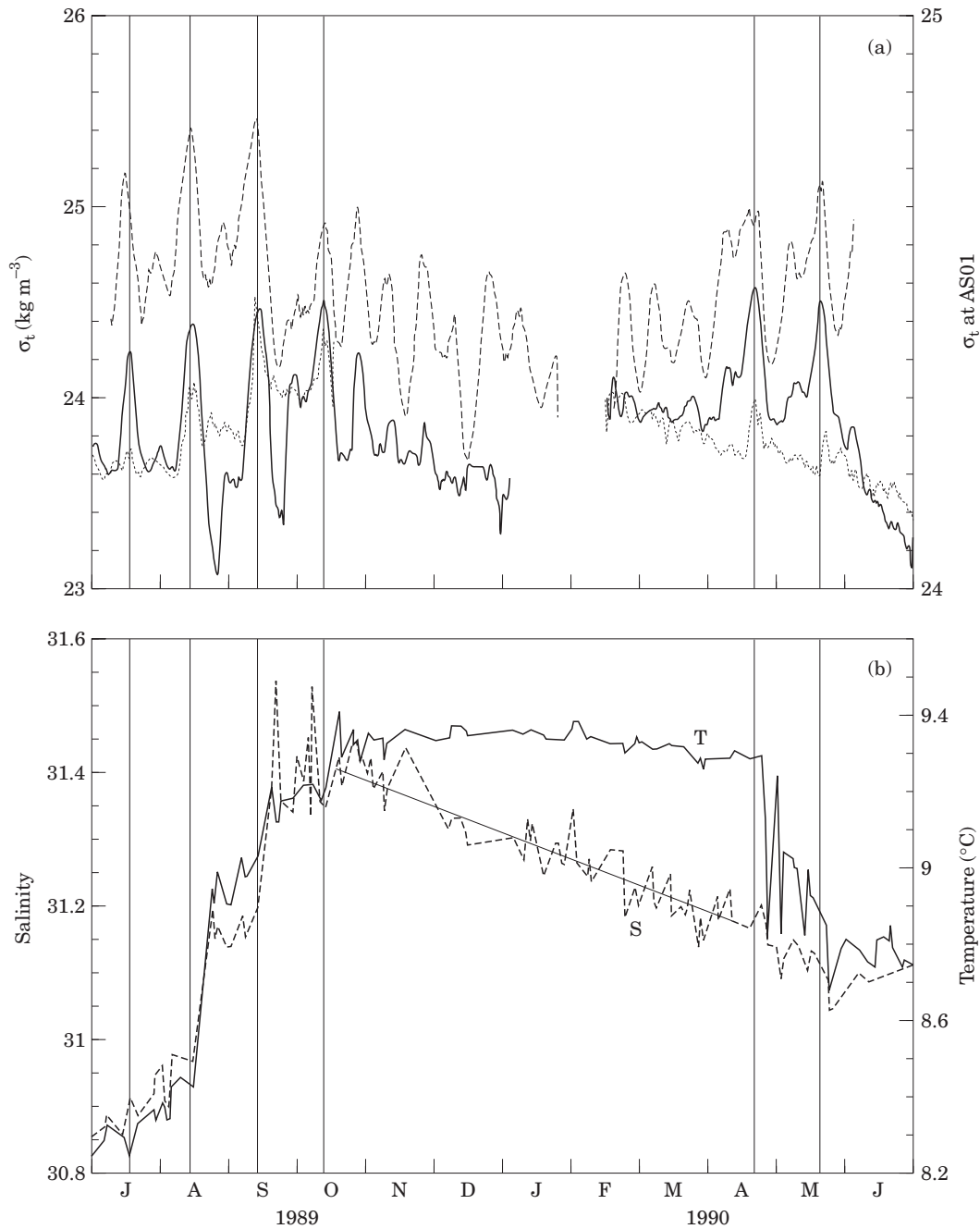
FIGURE 2. The upper panel (a) gives a time series of the density of the bottom water at AS02 (full line), AS03 (dashed line), and AS01 (dotted line). The density is given as $\sigma_t = (\rho - 1000)$ kg m^{-3}. Note the different density scale for AS01. The lower panel (b) gives the temperature and salinity measured near the bottom at NB. Salinity is given using the Practical Salinity Scale.

brings warm salty intrusions, and the spring season with the intrusion of colder water. In the fall, the increased salinity is responsible for the higher density of the intrusions. On the other hand, for the spring events, colder temperatures as well as slightly higher salinity both contribute about equally to the increased density. A close examination of the complete tempera-

ture time series from Nanoose Bay indicates that the period presented here is representative of a typical year (see Figure 11). Therefore, the combination of both the fall and spring deep water renewal seasons is responsible for establishing the yearly cycle for temperature and salinity of the deep water mass of the strait. This is characterized by a saw tooth cycle for
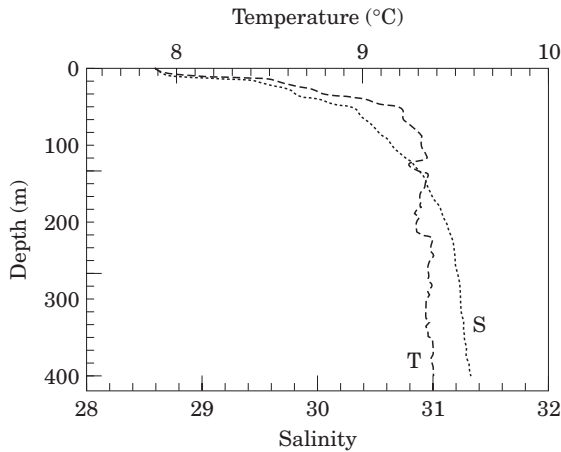
FIGURE 3. Vertical profile of temperature and salinity measured at the NB station on 2 January, 1990.

salinity with an abrupt increase in the fall followed by a gradual decrease over the rest of the year. Temperature varies in a step-like fashion with a low value plateau in summer and higher values in winter. A typical yearly T-S diagram for the deep water shows warm salty water in the fall, followed by gradual freshening through the winter, an abrupt cooling in the spring, and finally a return to warm and salty water in the subsequent fall (see Figure 4 of LeBlond *et al.*, 1991).

According to the yearly cycle of the bottom water properties described above, most of the water input into the deep basin comes during the spring and fall deep water renewal seasons. For the rest of the year, the deep water mass appears to diffuse slowly into the fresher layer above it. To examine this hypothesis, a simple diffusion model is applied to the water salinity data of Figure 2(b). In the case of temperature, as mentioned above, relatively small vertical gradients below the surface layer lead to a nearly isothermal deep layer through winter. Assuming an horizontally homogeneous deep central basin for which changes between deep water renewal seasons are due only to turbulent mixing, we have:

$$\frac{\partial S}{\partial t} = \frac{\partial}{\partial z}\left(K_z \frac{\partial S}{\partial z}\right) \qquad (1)$$

where K_z is the vertical eddy diffusivity, and $\partial/\partial t$ and $\partial/\partial z$ are the usual time and vertical derivatives of salinity S. Integrating this equation through the deep layer, extending from the bottom ($z = -H$) to a depth $z = -H + \Delta h$, leads to:

$$\int_{-H}^{-H+\Delta h} A(z)\frac{\partial S}{\partial t}\,\partial z = K_z A(z)\frac{\partial S}{\partial z}\Bigg|_{-H+\Delta h} \qquad (2)$$

with $A(z)$ the horizontal area at level z. An estimate of the vertical diffusivity K_z can be obtained from the data by calculating both derivatives and extracting $A(z)$ from depth contours on hydrographic charts. A linear fit to $\overline{S}(t)$, the mean salinity for water deeper than 300 m [Figure 2(b)], over the winter period of slow salinity decrease yields $\partial \overline{S}/\partial t \approx -14 \times 10^{-9}\ \mathrm{s}^{-1}$. Linear fits to $S(z)$ measured at various z levels within the deep layer give similar estimates for the time derivative. Therefore, $\partial \overline{S}/\partial t$ is used in Equation 2 as an estimate of $\partial S/\partial t$. To determine the vertical salinity gradient, 30 vertical profiles collected at station NB during the winter of 1989/90 have been used and a mean value of the vertical gradient determined (see Figure 3 for a typical profile). This leads to an estimate of $\partial S/\partial z \approx -11 \times 10^{-4}\ \mathrm{m}^{-1}$ at the top of the deep layer, chosen as $z = -300$ m. From these estimates the eddy coefficient takes a value of about $1 \cdot 1 \times 10^{-3}\ \mathrm{m}^2\ \mathrm{s}^{-1}$.

There are no direct measurements to corroborate this estimate. However, estimates derived from the same budget method applied to data collected in a nearby fjord (de Young & Pond, 1988), Indian Arm, gave similar values with a range of $0 \cdot 5 \times 10^{-3} \leq K_v \leq 15 \times 10^{-3}\ \mathrm{m}^2\ \mathrm{s}^{-1}$. Therefore, the above results are not inconsistent with the idea that the deep water mass slowly mixes with the fresher layer above it in between deep water renewal seasons. The resulting decrease in density of the deep water due to the diffusion of salt between DWR seasons plays an obvious role in the timing of these periods by predisposing the deep water for the next series of deep intrusions.

The two yearly episodes of bottom water replenishment also appear to regulate the amount of dissoved oxygen in the deep strait. Figure 4 gives monthly values of both temperature and dissolved oxygen, measured near the bottom of the deep central basin in the year 1968. The data were extracted from the Crean and Ages (1971) data set, using an average of the measurements taken below 300 m depth at two hydrographic stations located near NB. The cold water arriving in the spring contains a higher level of dissolved oxygen than the warmer water flowing in at the end of the summer, resulting in decreased amounts of dissolved oxygen during summer. Data from recent surveys also indicates that the cold (warm) deep water renewal events have low (high) level of nutrients.

The detailed structure of individual density intrusions is illustrated in Figure 5 where temperature, salinity, density, and along-isobath velocity are given as measured at both AS01 and AS02 during one fall and one spring renewal episode. All time series have
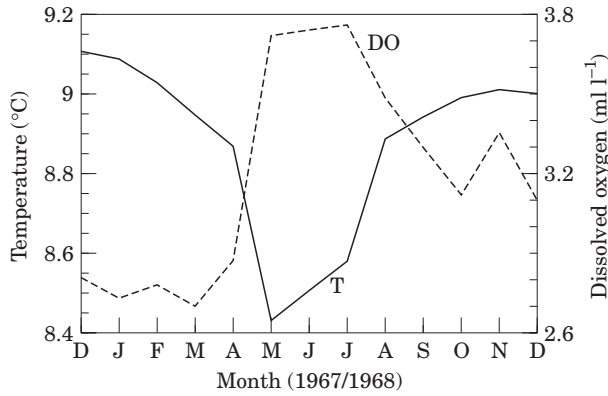
FIGURE 4. Average monthly values of bottom temperature (full line) and dissolved oxygen (dashed line) measured in the deep Strait of Georgia by Crean and Ages (1971).

been lowpass filtered with a 25 h running mean filter to suppress the dominant tidal signal. For each event, the passage of dense water at both locations is seen as an increase in salinity, density and velocity, first at AS02, and then at AS01. In the case of the temperature signal, the cold pulse at AS02 becomes, as it reaches AS01, a warm pulse for the fall event as opposed to a cold signal for the spring intrusion [Figure 5(a)]. Each event lasts about 10 d, with the amplitude of the signal decreasing from AS02 to AS01 as the dense water pulse is mixed with ambient water on its way into the deep basin. Each intrusion also displays the shape characteristic of a gravity current with a sharp forward front at the head followed by a more diffuse tail in the back where mixing is more intense (e.g. Benjamin, 1968). Although there is a temperature contrast associated with each pulse for both seasons, the density anomaly of the fall events is determined mostly by salinity.

In the case of late summer deep water events, a peculiar temperature signal is seen at AS01 [Figure 5(a)] with the temperature maximum preceding the density and velocity peaks by a few days. In late summer, contrary to the spring season, the temperature of the shallower water near the sill (AS02) is warmer than at AS01. When a pulse of cold salty water propagates from AS02 to AS01 it becomes a warm pulse relative to the colder water of the deep basin, with the stronger temperature contrasts at the front and back of the advancing pulse. For all deep water renewal events of the fall season, this results in a temperature peak at AS01 near the intrusion head, preceding the peak in density (salinity) and velocity associated with the core of the dense pulse. The more intense mixing in the back of the intrusion may be efficient in diluting the second

warm signal initially following the core. The resulting temperature signal associated with the passage of the dense pulse at AS01 then becomes a single sharp peak in the front of the pulse. A similar behaviour was observed in the summer/fall of 1984 for three deep water renewal events measured near the bottom of the Strait of Georgia (LeBlond et al., 1984, their figure 13) for which the temperature maxima preceded each density (and velocity) peak.

The results of Figure 5 can also be used to compare velocities measured within the intrusions to predictions of the gravity current theory. Benjamin (1968) derived an expression for the propagation speed, c, of a steady density current of thickness d in a two-layer system of constant total depth H:

$$c = \left[\frac{(H-d)(2H-d)}{H(H+d)} \right]^{\frac{1}{2}} \sqrt{g'd} \qquad (3)$$

where g' is the reduced gravity. At AS01, the water depth is $H=300$ m and, from Figure 5(c), we have $g' \approx 1.4 \times 10^{-3}$ m s^{-2}. The present data set does not allow a measure of the thickness of the intrusion but it seems reasonable to assume that typical values are about $d \approx 50$ m, as in LeBlond et al. (1991) and Geyer and Cannon (1982). From (Eqn 3), one obtains an estimate of the propagation speed $c \approx 30$ cm s^{-1}. This prediction is about twice the maximum Eulerian velocity measured in the core of the intrusion at AS01 [Figure 5(d)], but close to the one measured upstream at AS02. The propagation speed of the intrusions can also be estimated from the time it takes for the dense water to travel the 28 km distance from AS02 to AS01. For the two events of Figure 5, a time lag of 2 to 3 d gives a value of $10 \leq c \leq 15$ cm s^{-1}. The latter estimate is within the range of velocities values measured in the intrusions at AS01 and AS02. Although the above estimates do include many uncertainties (the thickness of the intrusions for example), they indicate that measured velocities are of comparable magnitude to values given by the two-layer gravity current theory. Similar results were obtained by Geyer and Cannon (1982) in the case of bottom intrusions into Puget Sound.

Evident in Figure 2(a) is the regular spacing of about a month between successive DWR events. This reflects the dependence of the process on the tidally induced fortnightly mixing over the sills mentioned by previous investigators (e.g. LeBlond et al., 1991). We now turn our attention to the close link between the fortnightly tidal modulation and the deep water renewal process.
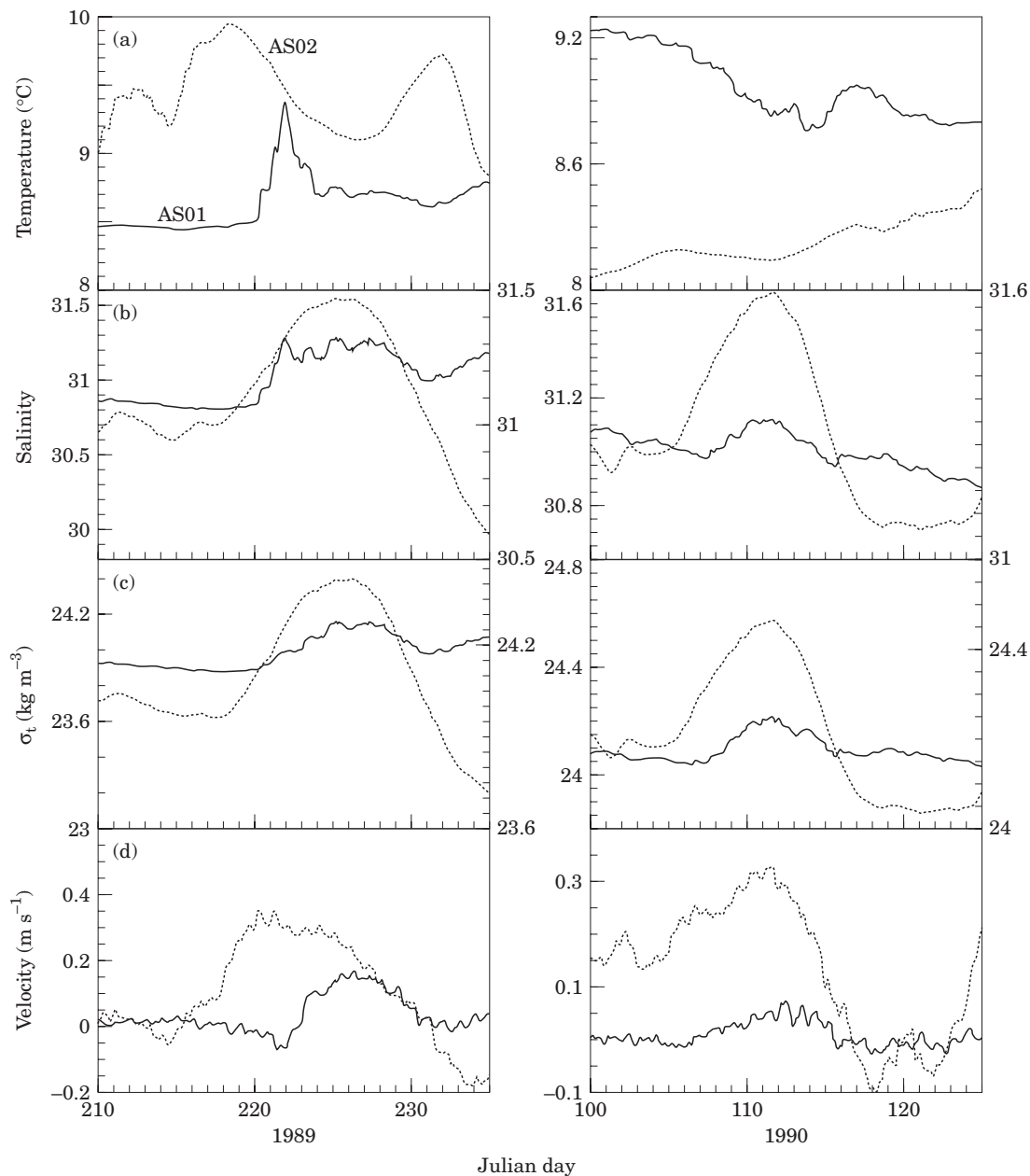
FIGURE 5. Lowpass filtered temperature (a), salinity (b), density (c), and along-isobath velocity (d) measured at AS01 (full line) and AS02 (dotted line) during a fall (left side panels) and a spring (right side panels) deep water renewal event. When different from AS02, the scale for AS01 is on the right hand side of the plots.

Fortnightly tidal forcing

Examination of the tidal velocities on Victoria sill (AS04) shows that each deep water renewal event happens in connection with a neap tide, at monthly intervals (Figure 6). In this figure, the periods of the six deep water intrusions are identified as the times for which elevated density values were present near the bottom at AS02. The tidal forcing is represented as the lowpass filtered cube-root mean cube (CRMC) of

the current (e.g. Griffin & LeBlond, 1990) measured at AS04. LeBlond et al. (1991) noticed a similar phase relation between dense pulses measured in 1984 along the bottom of the Strait of Georgia and tidal velocities at Boundary Pass. In particular, they observed that maximum currents along the bottom of the deep strait (at STN3, Figure 1) occur about 4 d after the smallest tidal currents at the pass. They interpreted these fluctuations as tidally modulated gravity currents entering the strait during the weakest
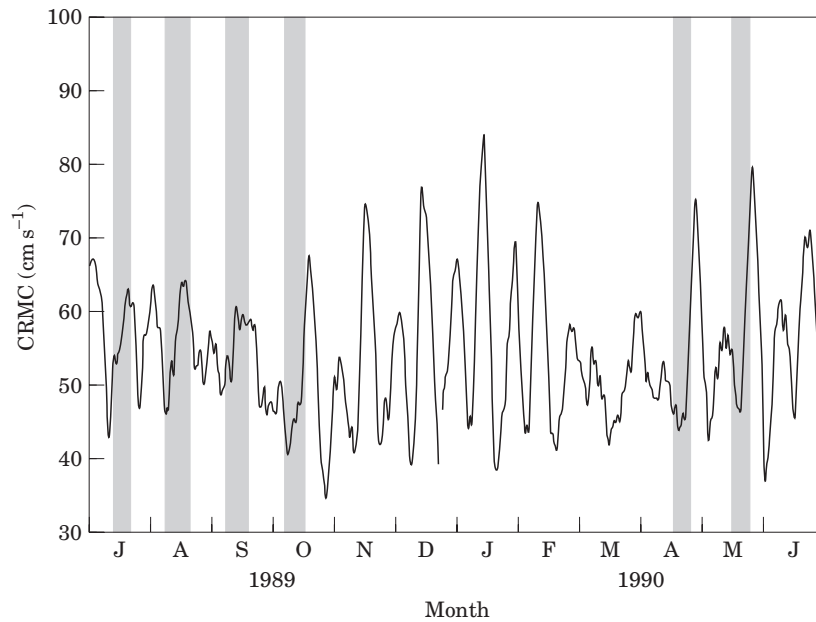
FIGURE 6. Cube root of the mean cube (CRMC) velocity near the bottom of Victoria sill (AS04), along with DWR events identified as time intervals of high water density at AS02 (shaded).

summer neap tides, when mixing is minimum at the sill.

LeBlond *et al.* (1991) also explain the fact that intrusions occur monthly, on every other neap tide, by suggesting that the tidally induced mixing in the Boundary Pass area controls the deep water exchange, allowing dense enough water to flow relatively unmixed only during the weakest of the two monthly neap tides. Accordingly, they suggest that there is a threshold level in the tidal current (about 50 cm s^{-1}) above which the deep flow penetration is cut off. To examine how well this concept applies to the 1989/1990 data set, the intensity of the tidal mixing at Boundary Pass (AS03) is given in Figure 7 in relation with the timing of the deep water renewal events. The cube of the measured velocities is used here as an index of the local rate of energy dissipation and mixing. The time interval for each intrusion is similar to those of Figure 6, except that they have been adjusted by a small lag of 1·5 d to reflect the approximate time needed to reach AS02 from AS03 at the advection speed of 30 cm s^{-1} reported in the previous section. In Figure 7, there is no evidence of a systematic link between minimum local mixing and periods of dense water intrusion. On the contrary, large velocities, and hence mixing, were present at Boundary Pass during many of the events (e.g. August 1989). Also included in the figure, is the time series of an estimate of density flux anomaly flowing over the sill, into the Strait of Georgia. The density flux

anomaly over Boundary Pass, Q, is computed as $Q=[v_{thalweg} \ \Delta\sigma_t]$, with $v_{thalweg}$ the component of velocity along the local orientation of the thalweg, and $\Delta\sigma_t=(\sigma_t - 23)$, a density anomaly from a background value of $\sigma_t=23$ kg m^{-3}. Except for some brief periods during winter when the estuarine circulation is weaker, the density flux remains well above zero, reflecting the persistent deep inflow into the strait. Importantly, the data clearly show that each of the intrusions corresponds to a local maxima of density flux at Boundary Pass. These large values of density influx are not necessarily concomitant with weak local tidal mixing. However, they do correspond to a monthly maxima in water density recorded near the bottom at the sill (see Figure 8).

Deep water renewal events thus appear to be directly triggered once a month by the availability of dense enough water near the sill, and not by a minimum in the local tidally induced mixing. The presence of denser water at the bottom of the sill once a month is obviously linked to the fortnightly variations in tidal mixing which have been shown to modulate strongly water properties in the vicinity of the sill (e.g., Griffin & LeBlond, 1990; Masson & Cummins, 2000). To examine this link, the CRMC and residual current measured at Victoria Sill (AS04) are given in Figure 8, in relation with bottom salinity at Boundary Pass (AS03) for the month of August 1989. During each neap tide when the CRMC at AS04 is lower, tidal mixing is reduced and, in
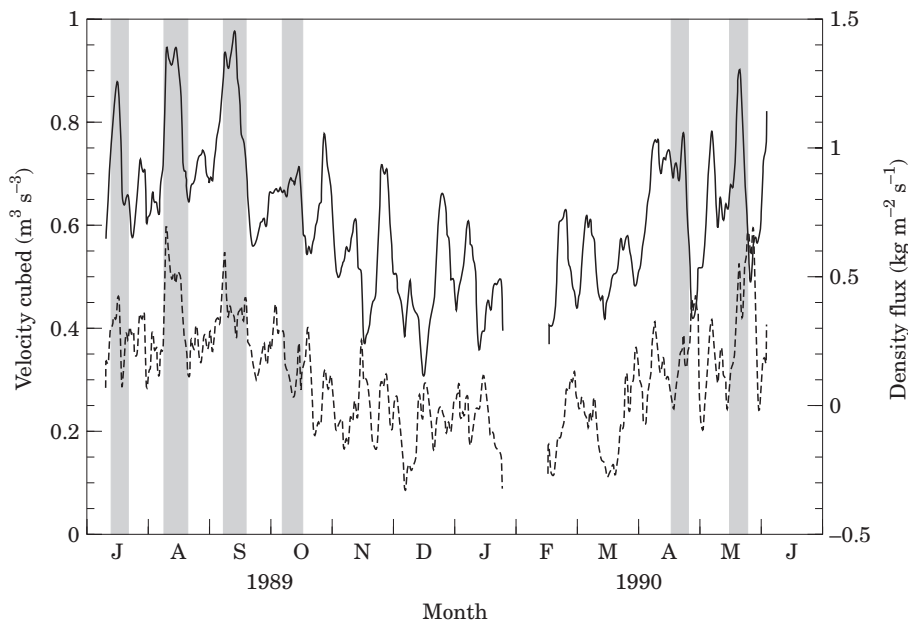
FIGURE 7. Lowpass filtered tidal mixing intensity at Boundary Pass (AS03) represented by the velocity cubed (dashed line), and density influx over the pass (full line). As in Figure 6, the DWR events are indicated as time intervals of large density recorded at AS02 but, this time, advanced by a 1·5 day time interval.
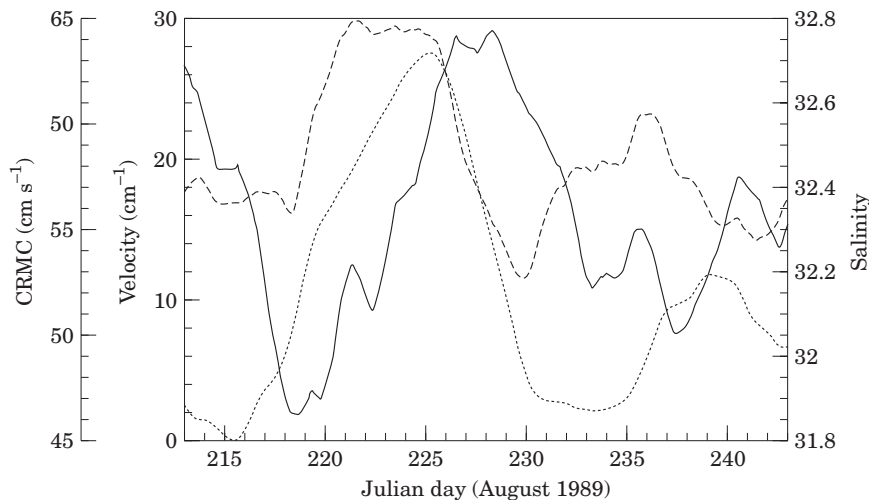

FIGURE 8. Residual current (dashed line) and CRMC (full line) measured at AS04 and bottom salinity (dotted line) measured at AS03 during the month of August 1989.

response, the estuarine circulation is enhanced due to the decreased vertical exchange of momentum (e.g. Park & Kuo, 1996). Meanwhile, the salinity at AS03 increases during neap tides to reach maximum values just after the end of a neap period, a few days following the period of minimum tidal currents. It is at this time (e.g. day 225 of Figure 8), when dense water is available near the sill, that the large values of density flux indicated in Figure 7 are recorded over the sill, and a deep intrusion is formed.

The observations described above suggest that each neap tide is followed by the presence of high density water near the bottom of the sill at Boundary Pass. However, the data also indicate that, after each deep intrusion, the density near the bottom of the sill decreases significantly as the denser water of the intrusion flowing into the strait is replaced by fresher (lighter) water (see Figure 2). It then appears to require two consecutive neap tides in order to bring the salinity near the sill to high enough values,
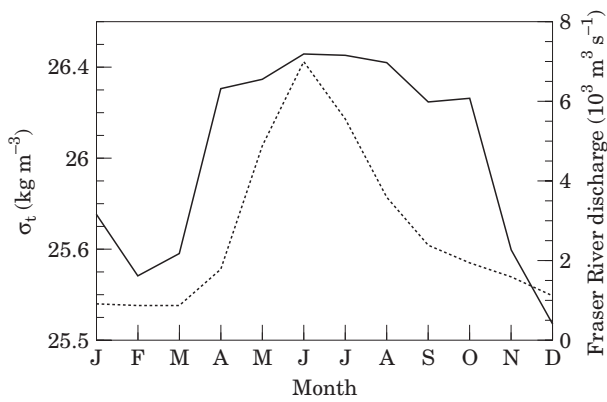
FIGURE 9. Mean monthly density, σ_t, near the bottom of Juan de Fuca Strait (full line) and mean monthly Fraser River discharge (dotted line).

resulting in the monthly periodicity for renewal events. This finding is in agreement with the previous work of Park and Kuo (1996) who found that, for large estuaries, the time response of the density field may be longer than the fortnightly forcing period. In this problem where the two sills form a middle intermediate basin (Haro Strait), this suggests that, during a single neap tide, the estuarine circulation cannot completely replenish the deep dense water mass in Haro Strait. Two fortnightly periods appear to be required.

Seasonal and interannual variability

In section 2, the seasonal cycle of water properties in the deep basin of the Strait of Georgia was shown to be linked closely to the two deep water renewal seasons. Several vigorous late summer events bring warm, saline, low oxygen water that is rich in nutrients into the deep basin. Late winter events transport cold, slightly saltier, high oxygen, low nutrient water. We now examine the timing of the two DWR seasons in relation to the annual cycle of water properties of both the estuarine surface outflow and deep return flow. The density of the deep water flowing into Juan de Fuca Strait is strongly modulated by the upwelling/ downwelling seasons on the shelf west of Vancouver Island. During the upwelling season (from about April to October), the deep estuarine return flow advects cold, salty, low oxygen, high nutrient water into Juan de Fuca Strait (e.g. Thomson, 1994). In Figure 9, mean monthly water density is given for the bottom water (below 100 m depth), in central Juan de Fuca Strait. The monthly mean values have been computed from a total of 1179 water samples collected in the middle section of Juan de Fuca Strait, over a 62-year period (1938–1999). In the spring, at the onset of the upwelling season, the density of the deep return flow in Juan de Fuca increases sharply, maintaining relatively high values through the summer season, up to the month of October.

As it travels inland, this dense water mixes to various degrees with the fresher surface estuarine outflow. In order for the resulting diluted bottom water to be dense enough at Boundary Pass to be able to flow to the bottom of the Strait of Georgia, the surface water with which it mixes cannot be too fresh. A similar dependence of deep water inflows on low river runoff rates has also been found in other fjords (e.g. Allen & Simpson, 1998). Surface water properties within the estuary are strongly determined by the annual cycle of the Fraser River, with much fresher surface water present during freshet. For a typical year, the freshet occurs during the summer season and extends from May through August, with peak discharge usually in June (Figure 9). These conditions lead to the two observed DWR seasons for which conditions of denser return flow and relatively low river discharge overlap. Such conditions develop both at the beginning (in the spring) and at the end (in early fall, August to October) of the upwelling season. Thus it appears that the timing of the deep water renewal seasons is determined by the ability to form dense enough water near the sill. This occurs when both the surface outflow and the deep return flow carry water of relatively high salinity.

The conditions described above would lead to a regular annual cycle for the water properties of the deep Strait of Georgia. However, year to year variability in both the upwelling season and river freshet can lead to important variations in timing and intensity of the deep water renewal seasons. In Figure 10 the bottom temperature for the deep Strait of Georgia (depths >300 m) is given as measured at the Nanoose Bay station since 1969. Evident in the time series is the warming observed around 1976, in agreement with the warming of coastal waters known to have occurred at that time in the North Pacific Ocean (e.g. McGowan, 1998). On a shorter time scale, the time series variability is dominated by the yearly cycle of cooling during the spring DWR season and warming at the end of the summer during the second annual DWR season. However, some years display marked departures from this typical pattern. During the year following the onset of a strong El Niño event, the temperature at the bottom of the strait is quite steady and does not show the typical spring cooling. In Figure 10, the vertical dashed lines highlight the first year of each of the six major El Niño events recorded during this period (1972, 1976, 1982, 1986, 1991,
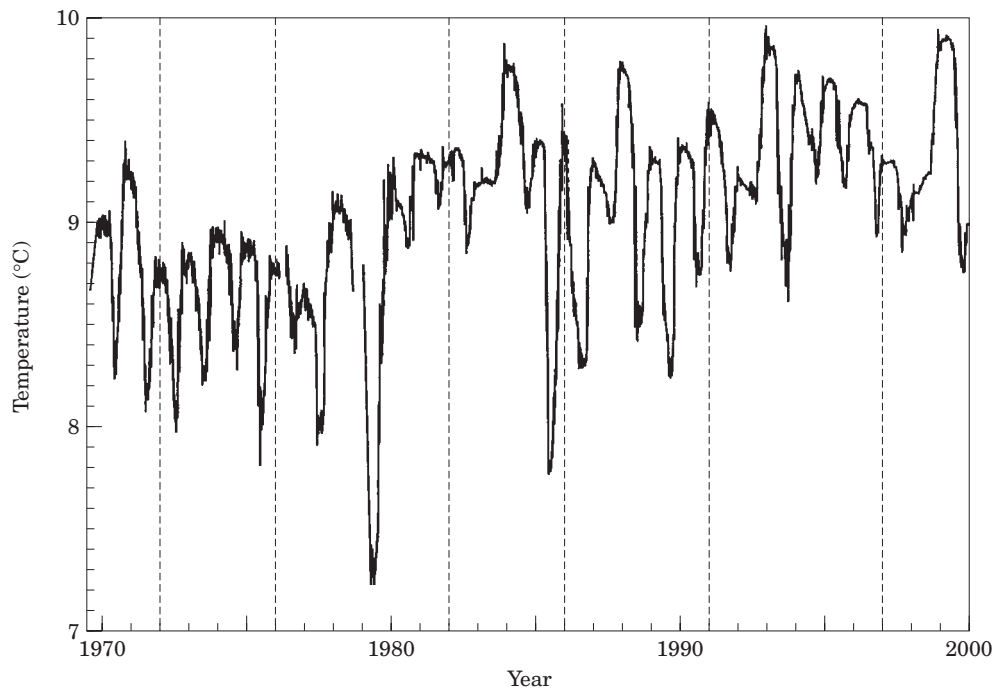
FIGURE 10. Bottom temperature at station NB. Dashed lines indicate beginning of major El Niño events.

and 1997). Except for the 1972 event which, despite being a strong tropical El Niño event, did not lead to significant warming at higher latitudes in the Pacific (Emery & Hamilton, 1985), the temperature signal for all years following the onset of a strong El Niño fails to display the characteristic marked cooling that normally takes place during spring in the deep strait.
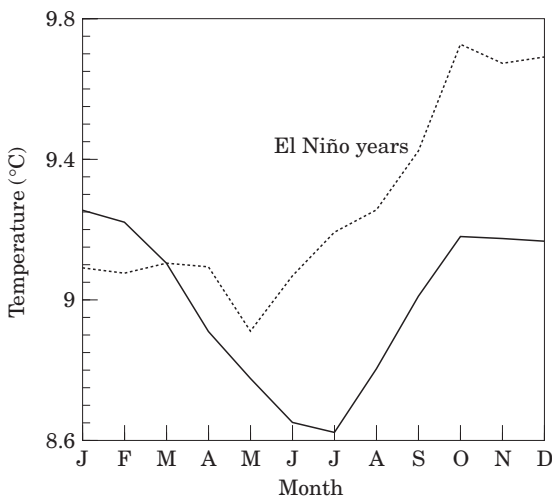

FIGURE 11. Comparison of the mean monthly temperature measured near the bottom at station NB for those years following the onset of a major El Niño (dotted line) with the mean of non-El Niño years (full line).

To demonstrate the anomalous cycle of the bottom temperature during El Niño years, mean monthly temperature has been computed for the year immediately following the onset of the five El Niño events affecting the area. This is compared in Figure 11 with the mean monthly values for the remaining years. In those five years, there was no strong spring cooling of the bottom water in the Strait of Georgia. The likely reason for this is that upwelling activity on the shelf off the west coast of Canada is weaker during winter and spring following the onset of strong El Niño conditions (e.g. Freeland & Thomson, 1999), resulting in anomalously warm, fresh water on the shelf. With weaker upwelling, the salinity of the deep return flow within Juan de Fuca Strait is lower and a consequent shutdown of the spring DWR season ensues. Following such a summer during which the deep water stays relatively warm, the fall DWR season subsequently raises the bottom temperature to relatively high values (Figure 11).

Conclusion

Several data sets were examined in order to better understand the deep water renewal process in the Strait of Georgia and the various time scales involved. It is found that deep water replenishment occurs episodically in the form of discrete intrusions with

characteristics similar to those of bottom gravity currents. They are grouped into two distinct seasons which regulate the yearly cycle of the deep water properties of the Strait of Georgia. In the spring, cold, nutrient depleted water with high dissolved oxygen content penetrates the deep basin. In contrast, during the fall, deep intrusions carry warm, saline water with low dissolved oxygen and high nutrient content. The strength and regularity of the deep water seasons could then have a significant impact on the ecosystem of the estuary through its influence on these various properties of the deep water mass. Between DWR seasons, the secular decrease of salinity of the deep water mass can be accounted for by the effect of turbulent diffusion and mixing with the layer above it.

DWR events are linked to the tidal fortnightly cycle with each event shown to occur following a neap tide, when the density near the bottom of the sill peaks. In addition, during DWR seasons, it is found that deep intrusions occur monthly, after every other neap tide. This appears to be controlled by the time response of the density field within the estuary being longer than the fortnightly tidal forcing. In other words, it is found that it takes two consecutive neap tides for the density at the sill to reach high enough values after the flushing of dense water by the previous DWR event.

The timing of the two DWR seasons is explained in terms of overlap of the coastal upwelling season and Fraser River freshet through the year. Also discussed is the large departure from the typical yearly cycle observed during strong El Niño events. During years following a major El Niño, the presence of fresher, warmer water on the shelf seems to shut down the spring DWR season, with water in the deep Strait of Georgia reaching unusually high values during the following fall DWR season.

Although the intent of this study has been to shed some light on various aspects of the deep water renewal process, certain effects have not been considered. For example, the influence of wind forcing on both the onset and strength of the deep intrusions has not been addressed. Cannon *et al.* (1990) have shown that, for Puget Sound in winter, while intrusions occur during neap tides, the onset of the deep intrusions can be controlled by density changes near the sill caused by wind storms on the Pacific coast. Such wind effects could also play a role in the Strait of Georgia DWR, especially during winter when the estuarine circulation is weaker and the wind stress generally stronger.

Acknowledgements

References

Allen, G. L. & Simpson, J. H. 1998 Deep water inflows to upper Loch Linnhe. *Estuarine, Coastal and Shelf Science* **47,** 487–498.

Benjamin, T. B. 1968 Gravity currents and related phenomena. *Journal of Fluid Mechanics* **31,** 209–248.

Birch, J. R. 1991 Deepwater renewal at neap tides in the southern Strait of Georgia, 1989–1990. Unpublished report by Arctic Sciences Ltd., Sidney, B.C. for the Institute of Ocean Sciences, 43 pp.

Cannon, G. A., Holbrook, J. R. & Pashinki, D. J. 1990 Variations in the onset of bottom-water intrusions over the entrance sill of a fjord. *Estuaries* **3,** 31–42.

Crean, P. B. & Ages, A. B. 1971 Oceanographic records from twelve cruises in the Strait of Georgia and Juan de Fuca Strait, 1968. Department of Energy, Mines, and Resources, Marine research sciences branch, Vol. 1–4, 389 pp.

de Young, B. & Pond, S. 1988 The deepwater exchange cycle in Indian Arm, British Columbia. *Estuarine, Coastal and Shelf Science* **26,** 285–308.

Emery, W. J. & Hamilton, K. 1985 Atmospheric forcing of inter-annual variability in the northeast Pacific Ocean: connections with El Niño. *Journal of Geophysical Research* **90** (C1), 857–868.

Freeland, H. & Thomson, R. 1999 The El Niño signal along the West Coast of Canada—Temperature, salinity and velocity. In *PICES scientific report No. 10*, Sidney, B.C., 151p., pp. 55–58.

Gade, H. G. & Edwards, A. 1980 Deep water renewal in fjords. In *Fjord Oceanography* (Freeland, H. J., Farmer, D. M. & Levings, C. D., eds). Plenum, New York, 453–489.

Geyer, W. R. & Cannon, G. A. 1982 Sill processes related to deep water renewal in a fjord. *Journal of Geophysical Research* **87** (C10), 7985–7996.

Griffin, D. A. & LeBlond, P. H. 1990 Estuary/ocean exchange controlled by spring-neap tidal mixing. *Estuarine, Coastal and Shelf Science* **30,** 275–297.

LeBlond, P. H., Ma, H., Doherty, F. & Pond, S. 1991 Deep and intermediate water replacement in the Strait of Georgia. *Atmosphere-Ocean* **29,** 288–312.

Marinone, S. G. & Pond, S. 1996 A three-dimensional model of deep water renewal and its influence on residual currents in the central Strait of Georgia, Canada. *Estuarine, Coastal and Shelf Science* **43,** 183–204.

Masson, D. & Cummins, P. F. 2000 Fortnightly modulation of the estuarine circulation in Juan de Fuca Strait. *Journal of Marine Research* **58,** 439–463.

McGowan, J. A., Cayan, D. R. & Dorman, L. M. 1998 Climate ocean variability and ecosystem response in the NE Pacific. *Science* **281** (5374), 210–218.

Park, K. & Kuo, A. Y. 1996 Effect of variation in vertical mixing on residual circulation in narrow, weakly nonlinear estuaries. *Coastal and Estuarine Studies* **53,** 301–317.

Stacey, M. W., Pond, S., LeBlond, P. H., Freeland, H. J. & Farmer, D. M. 1987 An analysis of the low-frequency current fluctuations in the Strait of Georgia, from June 1984 until January 1985. *Journal of Physical Oceanography* **17,** 326–342.

Thomson, R. E. 1994 Physical oceanography of the Strait of Georgia-Puget Sound-Juan de Fuca Strait system. In *Review of the Marine Environment and biota of Strait of Georgia, Puget Sound and Juan de Fuca Strait* (Wilson, R. C. H., Beamish, R. J., Aitkens, F. & Bell, J., eds). *Canadian Technical Report on Fisheries and Aquatic Sciences*, No. 1948, 36–100.

Waldichuk, M. 1957 Physical oceanography of the Strait of Georgia, British Columbia. *Journal of Fisheries Research Board of Canada* **14,** 321–486.